Targets for personalized treatment of conjunctival melanoma

Cao, J.

Chapter 3

Overexpression of EZH2 in conjunctival melanoma offers a new therapeutic target

Jinfeng Cao, Kelly C. S. Pontes, Renier C. Heijkants, Niels J. Brouwer, Arwin Groenewoud, Ekaterina Jordanova, Marina Marinkovic, Sjoerd. van Duinen, Amina F. A. S. Teunisse, Robert M. Verdijk, Ewa Snaar-Jagalska, Aart G. Jochemsen, Martine J. Jager

Submitted for publication

Abstract

Malignant melanoma of the conjunctiva (CM) is an uncommon but potentially deadly disorder. Many malignancies show an increased activity of the epigenetic modifier Enhancer of zeste homolog 2 (EZH2). We studied whether EZH2 is expressed in CM, and whether it may be a target for therapy in this malignancy. Immunohistochemical analysis showed that EZH2 protein expression was absent in normal conjunctival melanocytes and primary acquired melanosis, while EZH2 was highly expressed in 13 (50%) of 26 primary CM and seven (88%) of eight lymph node metastases. An increased expression was positively associated with tumor thickness (p=0.03). Next, we targeted EZH2 with specific inhibitors (GSK503 and UNC1999) or depleted *EZH2* by stable shRNA knockdown in three primary CM cell lines. Both pharmacological as well as genetic inactivation of EZH2 inhibited cell growth and colony formation, and influenced EZH2-mediated protein expression and cell cycle profile *in vitro*. The tumor suppressor gene *p21* was especially upregulated in CM cells after *EZH2* knockdown CM cells. Additionally, the potency of GSK503 against CM cells was monitored in zebrafish xenografts. GSK503 profoundly attenuated tumor growth in CM xenografts using a well-tolerated concentration. Our results indicate that elevated levels of EZH2 are relevant to CM tumorigenesis and progression, and that EZH2 may become a potential therapeutic target for patients with CM.

Key words: conjunctival melanoma, EZH2, histone methylation, cell death, zebrafish.

Introduction

Conjunctival melanoma (CM) is a rare malignancy on the ocular surface, showing an increasing incidence in Europe and the United States [1-3]. CM recur frequently after surgical removal and can lead to death due to metastases [4,5]. The melanoma-related death rate can reach 29% at 10 years [5,6]. Once distant metastases occur, there are few therapeutic options.

CM share many characteristics with cutaneous melanoma, such as the presence of *BRAF* or *NRAS* mutations, which respectively occur in 29% and 18% of CM, and lead to activation of the MAPK pathway [7]. We recently showed that BRAF inhibitors are effective on *BRAF*-mutated CM cell lines [8] and at least two patients have been treated with these drugs [9,10]. As resistance to these drugs may develop, there is a need for alternative targets. One option is to investigate drugs that affect proteins involved in epigenetic regulation. Many epigenetic processes are regulated through the polycomb repressive complex 2 (PRC2), and overexpression of one of its catalytic subunits, Enhancer of zeste homolog 2 (EZH2), has been observed in a broad spectrum of cancer types including cutaneous melanoma, breast cancer, and endometrial carcinoma [11,12]. EZH2 is a histone methyltransferase which catalyzes trimethylation of lysine 27 in histone H3 (H3K27me3); this leads to transcriptional silencing of many genes, including tumor suppressor genes, rendering *EZH2* a potential oncogene [13,14]. EZH2 is not expressed in the normal tissues of adults, except in actively dividing cells, such as stem cells [15]. Somatic mutations including gain-of-function alterations of *EZH2* have primarily been discovered in hematopoietic malignancies, but sporadic activating mutations have also been identified in 3% of cutaneous melanoma [16]. While EZH2 expression is not detectable in benign nevi, it is expressed in cutaneous melanoma cells, suggesting a role for EZH2 in melanoma progression [17]. Indeed, EZH2 depletion or inhibition has been shown to repress melanoma growth and metastasis in a murine model of cutaneous melanoma [17].

Drugs that target EZH2 have shown promising preclinical results, and some phase 1/2 clinical trials using small molecule inhibitors have been initiated for lymphoma [18]. These inhibitors also show strong growth inhibitory effects on *EZH2* wild-type lymphoma cells *in vitro* [19,20]. We propose that EZH2 may also be overexpressed in CM, as in many ways CM resembles cutaneous melanoma, and blocking EZH2 may therefore inhibit the growth of CM cells.

We show that EZH2 expression is absent in normal conjunctival melanocytes and primary acquired melanosis (PAM), but is elevated in primary tumors and metastases of CM patients. In addition, we reveal that pharmacological inhibition of EZH2 activity or genetic depletion of *EZH2* leads to robust anticancer effects *in vitro* and *in vivo*. These results indicate that targeting EZH2 may provide a novel therapeutic strategy against CM.

Materials and Methods

Study population

Paraffin-embedded tissue specimens of nine PAM, 26 primary CM and one lymph node metastasis were collected through archive of the Department of Pathology, Leiden University Medical Center, Leiden, from patients who had been diagnosed with conjunctival melanocytic lesion between 1990 and 2014. Paraffin-embedded material of seven lymph node metastases of CM were retrieved from the Department of Pathology of the Erasmus University Medical Center. All the specimens contained enough material for the study. Five normal conjunctival samples were obtained from uveal melanoma-containing enucleated eyes. The use of human materials was approved by the Ethical Committee Board of Leiden University Medical Center and waived by Erasmus University Medical Center because it was a retrospective and non-interventional study. The diagnosis was reviewed and the original slides were assessed according to the 7th edition of the AJCC TNM cancer staging [21].

Immunohistochemistry (IHC) staining and evaluation

Immunohistochemistry (IHC) was carried out as previously described [22]. In short, after 10m (minute) of hot (100°C) antigen retrieval in a microwave and 1h (hour) cool down at room temperature (RT), sections were blocked with normal goat serum (1:10, X0907; DAKO, Glostrup, Denmark) for 1h at RT, after which the slides were incubated with anti-EZH2 monoclonal antibody (1:100, 612667; BD Biosciences, The Netherlands) overnight at 4°C. Thereafter, the slides were incubated with a goat-anti-mouse secondary antibody (K4000; EnVision+ System- HRP, Labelled Polymer, Dako) at RT for 1h. The staining was visualized with NovaRED substrate kit (SK-4800; VECTOR Laboratories, USA) for 15m at RT. Slides were then counterstained with hematoxylin and mounted with Kaiser's glycerin. Human placental tissue served as the positive control. The isotype control was obtained by replacing the primary antibody with the mouse IgG1 reagent (X9031, DAKO). Evaluation was done by two independent observers (JC and EJ) in a blinded manner. In case of divergent scores, a consensus was reached by simultaneous evaluation. Images were taken using Philips Image Management System 2.2. A staining index (SI) system, evaluating both intensity (0 = no staining, 1 = weak, 2 = moderate, and 3 = strong) and percentage of cells with nuclear EZH2 staining (1 ≤10%, 2 = 11%–50%, and 3 ≥50%) was used [12,23]. Multiplying intensity and percentage produced total scores (0-9). After considering the distribution plots and number of cases, the median (SI=3) was set as the cut-off value between low expression and high expression, as previously described [12,23].

Cell lines, lentiviral transduction and chemical reagents

Human CM cell lines CRMM1 and CRMM2 were established by G. Nareyeck, Essen, Germany [24], and kindly provided by M. Madigan, Sydney, Australia. CM2005.1 was established by S. Keijser, LUMC, Leiden, The Netherlands [25]. Human cutaneous melanoma cell lines A375 and MEL93.05 were kindly provided by E. M. E. Verdegaal, LUMC, Leiden, The Netherlands. The media and methods of cell culture have been described before [8]. Two validated MISSION®shRNA constructs (TRCN0000040-075 and TRCN0000040-077, Sigma Aldrich, USA)

were used to silence EZH2. Control shRNA vectors from the same library target green fluorescent protein (GFP) (shc005) or luciferase (shc007). HEK293T were transfected with the shRNA constructs together with helper plasmids encoding HIV-1 gag-pol, HIV-1 rev, and the VSV-G envelope as described previously [26]. To determine virus titers, p24 antigen levels were determined using a HIV-1 p24 antigen enzyme-linked immunosorbent assay (ELISA) kit (ZeptoMetrix Corp., USA). The CM cell lines were transduced with a MOI (multiplicity of infection) of 2.0 for 16h in medium containing 8.0 μg/mL polybrene. Virus-containing medium was replaced with fresh medium containing puromycin (1 μg/mL) for 72h to select transduced cells. GSK503 (S7804) and UNC1999 (S7165) were purchased from Selleck Chemicals (Huissen, The Netherlands). All drugs were dissolved in dimethyl sulfoxide (DMSO) to obtain a stock solution of 20 mM.

Immunoblotting

Protein lysates were extracted using 1.5× SDS sample buffer (75mM Tris HCl pH 6.8, 3% SDS, 15% glycerol). SDS-PAGE was carried out by loading 15-20 μg of total protein lysate on Mini-PROTEAN TGX Precast Gels (4-15%, Bio-Rad). Proteins were blotted onto Polyvinylidene difluoride (PVDF) membranes (Immobilon-P, Millipore, USA). Next, the membranes were incubated overnight with primary antibodies diluted with Odyssey blocking buffer (927-5000; LI-COR, The Netherlands) at 4°C, and visualized using IRdye-680 or IRdye-800 secondary antibodies (LI-COR). Blots were scanned and analyzed with the Odyssey Infrared Imaging System (LI-COR). Alternatively, membranes were incubated with horseradish peroxidase (HRP)-conjugated secondary antibodies and bands visualized by autoradiography. Primary antibodies are listed in Supplementary Table 1.

Cell proliferation and colony assay

The In-cell western assay was used to determine the growth rate, as previously described [8]. In brief, cells were seeded in triplicate in 96-well plates. EZH2 inhibitors at different concentrations were added 1 day later. After 5-day treatment

(pharmacological EZH2 inhibition), or treatment at day 1, day 4 and day 7 (*EZH2* knockdown), the cells were fixed in 4% formaldehyde and stained with DRAQ5 (1:7000, DR50050, Biostatus Ltd.). For a colony assay, cells were seeded in triplicate in 6-well or 12-well plates. Drugs at different concentrations were added 24h later. Medium was replaced with or without drugs every 4 days. After a 2-week incubation, cells were fixed in 4% formaldehyde and stained with 0.05% crystal violet. The plates were scanned with the Odyssey Infrared Imaging System.

Flow cytometry

Harvested cells were washed in cold PBS, fixed in 70% ethanol and stored at -20°C. Afterwards, cells were washed in PBS and resuspended in 2% fetal bovine serum/PBS with 50 μg/ml propidium iodide and 50 μg/ml RNase. Cell cycle analysis was carried out using BD LSR II system (BD Biosciences) and FACSDiva software (BD Biosciences).

RNA isolation, cDNA synthesis and real-time quantitative PCR (qRT-PCR)

RNA was isolated using the SV total RNA isolation kit (Promega, USA), after which cDNA was synthesized using the reverse transcriptase reaction mixture as indicated by Promega. qRT-PCR was performed using SYBR green mix (Roche Diagnostics, USA) in a C1000 touch Thermal Cycler (Bio-Rad laboratories, USA). Levels of *p14ARF*, *p21/CDKN1A*, *p16INK4a* and *p27KIP1* mRNAs were determined, corrected for housekeeping genes CAPNS1 and SRPR. The primer sequences are shown in Supplementary Table 2.

Fluorescent cell labeling and zebrafish model

To generate CM cells with red fluorescence, cells were stably transduced with lentivirus expressing both tdTomato and Blasticidin-S, as previously described [27]. Virus-containing medium was replaced with fresh medium containing Blasticidin-S (2 μg/mL) to select transduced cells. Transduction of the cells with the tdTomato-expressing virus did not alter the growth pattern of parental cells.

The (fli: GFP) Casper zebrafish embryos were maintained according to standard protocols (http://ZFIN.org, in the public domain) [28,29], in compliance with the Dutch animal welfare regulations. The research followed the statement on the use of animals in research as published by the Association for Research in Vision and Ophthalmology and was described previously [30]. To test drug toxicity, non-injected 3dpf (fli: GFP) Casper zebrafish embryos were put in a 24-well plate; each well contained 1ml of egg water, and different concentrations of GSK503. Six embryos were put into each well, maintained at 34°C, and monitored daily until 8dpf. The test was performed in triplicate and the media were refreshed every second day. When the survival was equal or higher than 80%, the concentration was considered nontoxic to the embryos.

After choosing the appropriate concentration, the same experimental conditions were applied for the treatment of tumor-cell injected embryos. Thus, at 2dpf, 350 to 450 cells of CRMM1, CRMM2, or CM2005.1 cells were injected inside the duct of Cuvier of (fli: GFP) Casper zebrafish embryos. At 1dpi, drug treatment was started and continued until 6dpi, completing a 5-day treatment. At 1dpi and 6dpi, injected embryos were anaesthetized with 0.160mg/ml tricaine (Sigma-Aldrich) to facilitate imaging under a stereo fluorescence microscope (Leica M205FA, Leica Microsystems, Inc.). The red pixels representing the number of cells inside the embryo were counted using Image J software (Schneider *et al*, 2012).

Statistical analysis

Statistical analyses were performed with either SPSS version 23.0 software (SPSS, Inc., USA) or R version 2.15.1 [31]. Pearson's chi-square, Fisher's exact and Mann-Whitney U tests were used for comparing categorical or numerical data of clinico-pathological characteristics. Two-tailed p values ≤ 0.05 were considered statistically significant. The plots of cell proliferation and cell cycle profiles were made with GraphPad Prism 6 software (La Jolla, USA). IC_{50} of drugs was calculated with CompuSyn software, according to relative 5-day growth inhibition [32]. The effect of GSK503 *in vivo* was analyzed using a generalized linear model after square-root transformation of the data.

Results

EZH2 is overexpressed in CM

We determined EZH2 expression in CM with IHC staining, analyzing the intensity and percentage of positive cells. Representative samples of different EZH2 expression patterns in CM are shown in Figure 1 (clinicopathological characteristics in Table 1, and clinical information in Supplementary Table 3). In normal conjunctiva, we observed some nuclear staining of keratinocytes, but not of melanocytes. EZH2 was also negatively expressed in PAM tissues (Supplementary Table 4). In contrast, EZH2 was highly expressed in 13 (50%) of the CM specimens, and was absent or marginally expressed in the other 13 (50%) primary CMs. In addition, seven (88%) out of eight lymph node metastases of CM showed strong EZH2 expression (Supplementary Table 5). In primary tumors, EZH2 expression positively correlated with tumor thickness (p=0.03). A high EZH2 expression was correlated with worse overall-survival and tended to associate with worse melanoma-related survival (Supplementary Figure 1). However, EZH2 expression was not correlated with tumor location, tumor stage, local recurrence, or distant metastasis (Table 1).

Pharmacological inhibition of EZH2 in CM cells

We determined EZH2 protein expression in three CM cell lines, a cutaneous melanocyte cell culture (07-11), and two cutaneous melanoma cell lines, one of which (A375) has previously been used extensively in determining the function of EZH2 [33]. Compared to the normal cutaneous melanocytes, all melanoma cell lines overexpressed EZH2 (Figure 2A). To investigate a putative growth stimulatory function of EZH2 in CM we treated the cells with small molecule EZH2 inhibitors GSK503 and UNC1999, since these had been shown to successfully inhibit the function of EZH2 in lymphoma and cutaneous melanoma *in vitro* and *in vivo* [17,34].

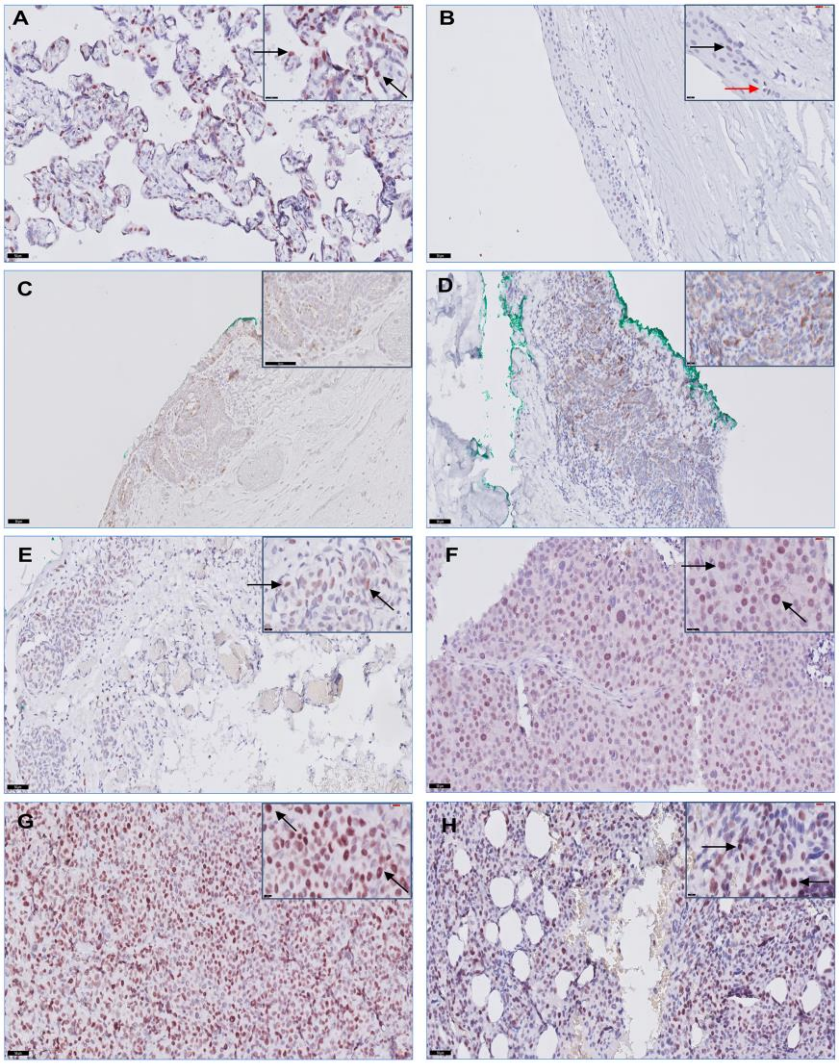

Figure 1. **Representative images of EZH2 IHC staining in CM**. (**A**) Positive control staining of placental tissue. (**B**) EZH2-positive keratinocytes (black arrow), and EZH2-negative melanocytes in the normal conjunctiva (red arrow). (**C**) EZH2 is absent in primary acquired melanosis. (**D**) CM with negative nuclear staining in all tumor cells. (**E**) CM with weak, (**F**) moderate, or (**G**) strong nuclear staining in >50% of tumor cells. (**H**) Strong nuclear staining in tumor cells in a lymph node metastasis. D and E were considered EZH2 low expression (scored ≤3); F, G and H were scored >3 and considered EZH2 high expression. Scale bar is 50μM in the original images. Black arrows indicate EZH2 positive cells.

Table 1. Clinicopathological characteristics according to low and high EZH2 expression.

	All cases	**EZH2 low**	**EZH2 high**	**Significance**
Characteristic	*Cases (%)*	*Cases (%)*	*Cases (%)*	*p value*
Overall	**26 (100)**	**13 (50)**	**13 (50)**	
Sex				
Male	11 (42)	8 (62)	3 (23)	*0.05**
Female	15 (58)	5 (38)	10 (77)	
Age at diagnosis				
Median [range], years	60.3 [21.2-86.3]	56.5 [21.2-73.0]	67.1 [48.7-86.3]	*0.03***
Tumor size, thickness	***N=23***	***N=11***	***N=12***	
Median [range], mm	1.0 [0.1-16.0]	0.6 [0.2-2.5]	3.3 [0.1-16.0]	*0.03***
Tumor size, LBD	***N=23***	***N=13***	***N=10***	
Median [range], mm	10.0 [2.0-30.0]	9.0 [2.0-30.0]	11.0 [5.0-20.0]	0.45**
Location				
Epibulbar	19 (73)	11 (85)	8 (62)	0.38&
Non-epibulbar	7 (27)	2 (15)	5 (38)	
cTNM				
T1	19 (73)	11 (85)	8 (62)	0.38&
T2	7 (27)	2 (15)	5 (38)	
Local recurrence				
No	16 (62)	7 (54)	9 (69)	0.42*
Yes	10 (38)	6 (46)	4 (31)	
Distant metastasis				
No	23 (88)	12 (92)	11 (85)	1.00&
Yes	3 (12)	1 (8)	2 (15)	

Abbreviation: LBD = largest basal diameter, cTNM = clinical TNM stage, based on the first occurring conjunctival melanoma. P value calculation: * = Pearson's chi-square; ** = Mann-Whitney U test; & = Fisher's exact test. Italic p values ≤ 0.05. Scoring method for EZH2 is described in the material and methods.

Figure 2B and 2F show that the level of H3K27me3 in CM cells decreased following increasing concentrations of GSK503 and UNC1999. EZH2 expression in CRMM2 and CM2005.1 was slightly decreased by GSK503, and UNC1999 clearly reduced EZH2 expression in CRMM2 at a high dose (6μM). IC_{50} values are shown in Table 2.

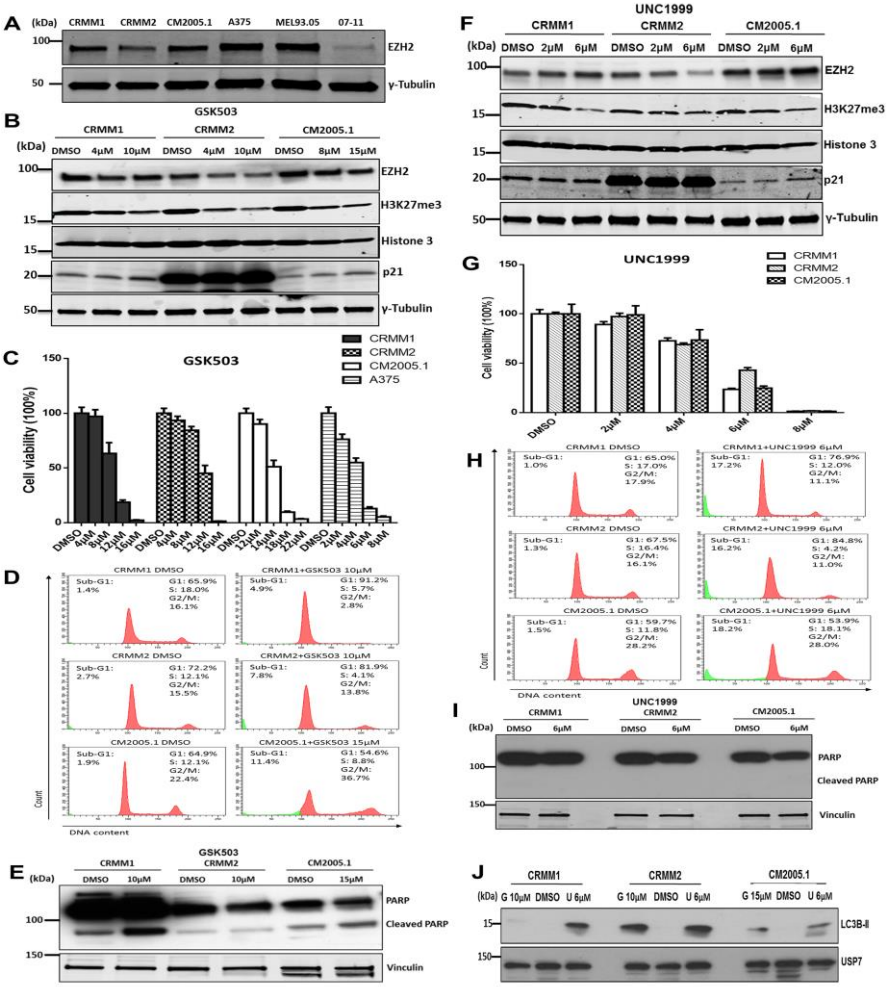

Figure 2. Effect of the EZH2 inhibitors GSK503 and UNC1999 on CM cell lines. (**A**) Western blot analysis of EZH2 protein in a panel of cell lines: CRMM1, CRMM2 and CM2005.1 are CM cell lines, A375 and MEL93.05 are cutaneous melanoma cell lines; 07-11 is a human melanocyte culture. Western blot analysis of CM cells upon 120h GSK503 (**B**) or UNC1999 (**F**) treatment. Representative bar graphs show the proliferation of melanoma cell lines exposed for 120h to GSK503 (**C**) or UNC1999 (**G**), respectively. The intensity (Y axis) was normalized to DMSO-treated control cells. Data were presented as means ± SEM (standard error of the mean), from one representative experiment. Histograms representing DNA content (**D, H**) and western blot analysis of (cleaved) PARP (**E, J**) following 120h incubation of GSK503 or UNC1999, respectively. (**J)** LC3B-II levels are increased following 120h incubation of GSK503 (G) or UNC1999 (U).

It has been reported that *EZH2* depletion increases p21 expression in cancer cell lines, and thereby induces cellular senescence [35,36]. Therefore, we examined p21 expression after drug treatment. However, we found that the p21 protein levels were only marginally elevated in CRMM1 and CM2005.1 cell lines exposed to either drug. Basal levels of p21 are very high in CRMM2 and the increase is hard to evaluate. Treatment for 5 days with GSK503 reduced the relative survival of CM cells, although the inhibitory effects on CM2005.1 cells required higher concentrations than the other cell lines (Figure 2C). Similarly, the proliferation of all CM cell lines was suppressed following UNC1999 treatment (Figure 2G). The colony formation assay confirmed the findings of the cell growth assay (Supplementary Figure 2).

Genes like *p14ARF*, *p16INK4a*, *p21/CDKN1A* and *p27KIP1* have been described as targets of EZH2 inhibition in several cancer types [35,37]. We therefore investigated whether GSK503 or UNC1999 affected the transcription of these genes in CM cells. However, mRNA expression of *p14ARF*, *p16INK4a*, *p21/CDKN1A* or *p27KIP1* was not significantly affected by these drugs (Supplementary Figure 3). However, results show that CM2005.1 does not express *p14ARF* nor *p16INK4a*, while CRMM2 lacks *p16INK4a* expression.

To determine the effects of EZH2 inhibition on cell cycle and apoptosis, we performed flow cytometry analysis after propidium Iodide staining (Figure 2D, 2H) and western blot analysis to investigate PARP cleavage (Figure 2E, 2I). Flow cytometry analysis of GSK503-treated CRMM1 and CRMM2 cells demonstrated a G1 arrest concomitant with S phase-depletion and slightly increased numbers of sub-G1 cells. In CM2005.1, on the other hand, we noticed an increase in the proportion of cells in G2/M phase (Figure 2D), also with an increase in the sub-G1 fraction. Some cleaved PARP could be detected in lysates from treated CRMM1 and CM2005.1 cells (Figure 2E). Following UNC1999 treatment, CRMM1 and CRMM2 cells showed an S-phase reduction concomitant with an increase of G1-phase cells. Furthermore, more sub-G1 cells were observed, indicating cell death (Figure 2H). In CM2005.1 cells, UNC1999 exposure did not have a strong effect on the cell cycle profile, but possibly the cells progress more slowly through S-phase since that

fraction is somewhat increased. A clearly increased sub-G1 fraction was identified, again indicating cell death. After UNC1999 treatment, no upregulation of cleaved PARP was observed in any cell line (Figure 2I), which may indicate that the observed cell death is not via induction of apoptosis. Since EZH2 has also been linked to the regulation of autophagy [38], the lysates of the three CM cell lines treated for 5 days with GSK503 or UNC1999 were investigated for expression of LC3B-II, a hallmark of autophagy [39]. Protein expression of LC3B-II was increased in CM cells upon GSK503 and UNC1999 treatment, although at different levels (Figure 2J), suggesting the induction of autophagy.

Table 2. Cell growth IC_{50} of EZH2 inhibitors in CM cell lines.

Cell line	GSK503 (μM)	UNC1999 (μM)
CRMM1	8.5±0.4	4.2±0.3
CRMM2	9.3±0.7	4.1±0.4
CM2005.1	15.9±1.4	4.4±0.3

Cell viability IC_{50} values of GSK503 (n=3) and UNC1999 (n=2) in CM cell lines (In-cell western assay) were determined based on relative 5-day survival.

Effect of *EZH2* knockdown in CM cells

Next, to genetically validate the findings of catalytic EZH2 inhibitors, we specifically depleted *EZH2* in melanoma cell lines using lentivirally-expressed short hairpin RNAs (shRNAs). Expression of EZH2 was significantly decreased in sh-*EZH2* expressing cells compared to control transduced cells (shc002, shc007), correlating with a global decrease of H3K27me3 (Figure 3A). This confirms that H3K27me3 is largely dependent on the presence of EZH2. Depletion of *EZH2* increased p21 protein levels in CRMM1, CRMM2 (shEZH2 20) and CM2005.1, suggesting that the cellular senescence marker *p21* participates in growth repression of CM cell lines. Activation of p21 transcription was detected in most *EZH2*-depleted cells, although some variation between cell lines and *EZH2* shRNAs was

observed (Figure 3B). We also investigated mRNA expression of *p16*, *p14ARF* and *p27*, but their expression was not affected by *EZH2* depletion (data not shown).

Importantly, the In-cell western assay indicated a lower proliferation of EZH2 shRNA-treated cells compared to control shRNA-treated cells (Figure 3C). Knockdown of *EZH2* also strongly decreased the ability of CM cells to form colonies (Supplementary Figure 4). Flow cytometry analyses showed that in CRMM1 and CRMM2, *EZH2* knockdown resulted in a S-phase depletion with G1 arrest (Figure 3D). Interestingly, in CM2005.1, *EZH2* depletion mainly caused an accumulation of cells in G2/M. In addition, an increased sub-G1 fraction was observed in all *EZH2*-depleted cells, suggesting that EZH2 protects CM cells from cell death.

Western blot showed that *EZH2* knockdown increased the amount of cleaved PARP in CM cell lines. It should be noticed that the full length PARP expression in CRMM2 cells upon *EZH2* depletion was strongly reduced, which may suggest that PARP is cleaved and that the cleaved product is unstable. In general, *EZH2* depletion induced some degree of apoptosis in CM cells, indicating its importance in cell survival. The results obtained upon *EZH2* depletion are strongly reminiscent of the data obtained with the GSK503 inhibitor (Figure 2D, 2E), suggesting that this inhibitor indeed mainly acts through inhibition of EZH2 activity, while UNC1999 might have additional activities [40].

Therapeutic effect of GSK503 in a zebrafish model

To confirm the findings obtained in cell culture, we established a zebrafish model to test the drug GSK503 *in vivo*. A well-tolerated concentration of GSK503 was determined as previously described [41]. Concentrations of GSK503 were nontoxic to the embryos till at least 8 days post-fertilization (dpf, Supplementary Figure 5), as over 80% of the embryos survived during the observation period, even at the highest concentration (24μM). Subsequently, three CM cell lines expressing tomato red were injected into the duct of Cuvier of (fli: GFP) Casper zebrafish embryos at 2dpf, and treatment with 24μM of GSK503 or DMSO diluted in egg water was initiated at 1-day post injection (dpi) and continued until 6dpi (5-day treatment). Next, cell growth

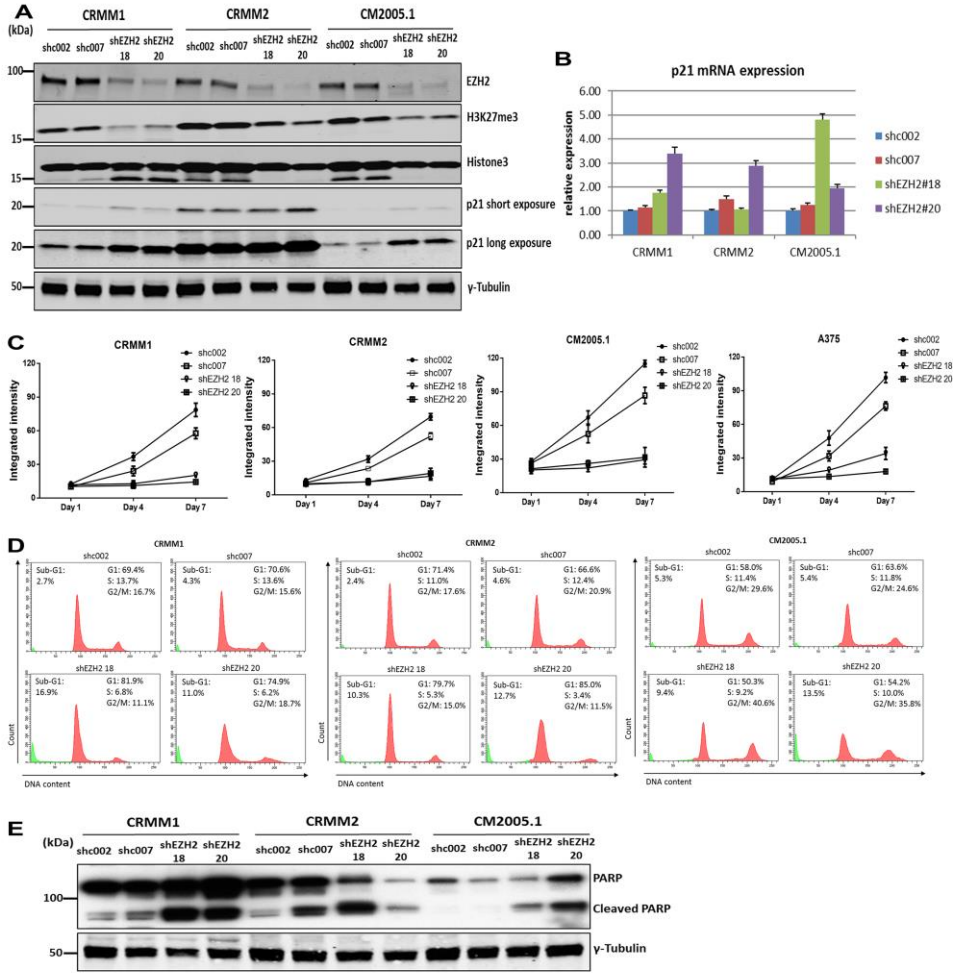

Figure 3. EZH2 knockdown reduces H3K27me3, elevates p21 expression, suppresses cell growth and induces cell cycle arrest and apoptosis in CM. (**A**) The expression of EZH2, H3K27me3, and cell cycle regulatory protein p21 was determined upon EZH2 depletion using (shEZH2 18, shEZH2 20) compared to control shRNAs (shc002 and shc007) 72h after puromycin selection. (**B**) The mRNA expression of p21 was elevated upon EZH2 knockdown. (**C**) Representative growth curves of CM cell lines and the A375 cell line after EZH2 knockdown by specific EZH2 shRNAs compared to control shRNAs. Error bars indicate the standard deviation. (**D**) Histograms show the percentages of CRMM1, CRMM2 and CM2005.1 cells in specific cell cycle phases, and western blot analysis (**E**) of (cleaved) PARP in CM cells upon EZH2 knockdown.

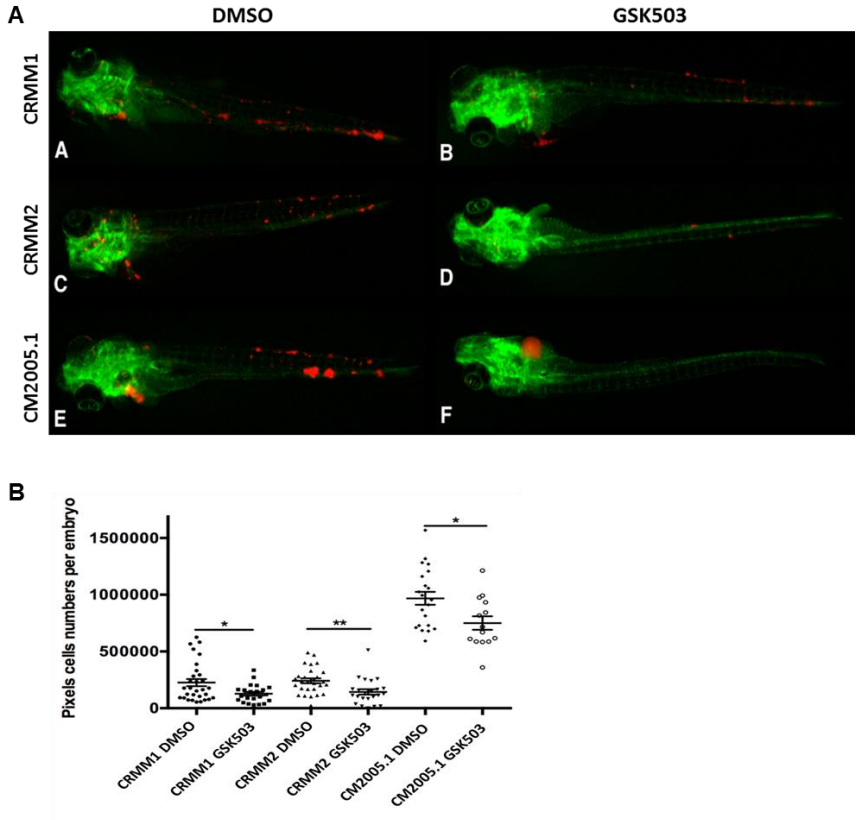

Figure 4. **GSK503 suppresses the cell growth of CM cell lines in the zebrafish model**. CM cells were labeled with tomato red (red) and injected into the duct of Cuvier at 2dpf in (fli: GFP) *Casper* zebrafish embryos which have a green vasculature. The images were taken at 6dpi. (**A**, black) Representative stereo fluorescent images (original magnification: 20x) show inhibition of tumour growth after exposure to 24μM GSK503. (**B**, black) Number of red pixels that represent tumour cells with DMSO or GSK503 treatment in CM xenografts. Each point indicates one embryo and its corresponding pixel count. Statistical significance was calculated by the generalized linear model and *p* values are indicated as follows: **p*< 0.05, ***p*< 0.01. $N_{CRMM1/DMSO}$= 30, $N_{CRMM1/GSK503}$= 22, $N_{CRMM2/DMSO}$= 28, $N_{CRMM2/GSK503}$= 23, $N_{CM2005.1/DMSO}$= 25, $N_{CM2005.1/GSK503}$= 18.

and dissemination were scored by counting the number of red pixels in the embryos. Figure 4 shows that tumor cells migrated to other areas through the blood circulation and proliferated. Importantly, the tumor burden of all three CM cell lines *in vivo* was significantly reduced after 5-day treatment with GSK503. We tested the difference

between the control and treated groups of the zebrafish embryos injected with three CM cell lines with a generalized linear model: the *p* values were 0.015 (CRMM1), 0.002 (CRMM2) and 0.028 (CM2005.1).

Discussion

To the best of our knowledge, this is the first study which demonstrates the importance of EZH2 in CM. Here we report the overexpression of EZH2 in CM. EZH2 was expressed on keratinocytes of normal conjunctiva, but not on cells of melanocytic lineage. This is consistent with studies of cutaneous melanoma, which similarly showed that EZH2 is present in epidermal keratinocytes, but absent or very low expressed in nevi and epidermal melanocytes [17,42]. Interestingly, although many CM develope in association with PAM [4], EZH2 was not expressed in PAM. Importantly, we demonstrate that EZH2 expression is detected in a significant proportion of CMs and is positively associated with one of the prognostic factors, tumor thickness [4]. Furthermore, EZH2 was highly expressed in most lymph node metastases. Taken together, our findings indicate that EZH2 protein levels are often increased in CM and metastases, and EZH2 may therefore be involved in the pathogenesis and progression of CM tumors.

Many small molecule inhibitors targeting EZH2 have been developed to block its catalytic activity, i.e. EZH2-mediated methylation of H3K27. A phase 1/2 clinical trial of Tazemetostat (EPZ-6438) is now ongoing against advanced solid tumors and B-cell lymphoma (NCT 01897571). In the present study, we applied two EZH2 inhibitors, GSK503 and UNC1999, on CM cell lines. In addition, we utilized genetic knockdown to confirm the findings of the pharmacologic depletion of *EZH2*. Interestingly, the tumor suppressor gene *p21* was more convincingly upregulated in *EZH2* knockdown CM cells than in inhibitor-treated cells, possibly suggesting that EZH2 has function(s) in transcription regulation independent of its catalytic activity. It is known that the mechanisms of EZH2 oncogenic activity are cancer type-dependent, including the canonical role of EZH2 in gene silencing in cutaneous

melanoma and colon cancer, and the non-canonical function of EZH2 that affects other pathways in a histone methylation-independent manner. For example, EZH2 can trigger NF-κB signaling in basal-like breast cancer, and can transcriptionally co-activate the androgen receptor in castration-resistant prostate cancer [43,44]. Further studies are warranted to elucidate the function(s) of EZH2 in CM. Regarding the cell cycle profile and apoptosis, drug treatment and RNA-interference (RNAi) similarly resulted in G1 arrest and S phase depletion in CRMM1 and CRMM2. GSK503 and UNC1999 appeared to induce cell death via partly different mechanisms. Similar to the genetic depletion of *EZH2*, the GSK503 inhibitor activated apoptosis and possibly some autophagy. However, increased caspase activity as monitored by PARP cleavage could not be detected upon UNC1999 treatment, but autophagy might be induced. Different patterns of cell death displayed by these treatments suggest that pharmaceutical inhibition cannot totally mimic the *EZH2* knockdown in this scenario. Discrepancies between genetic knockdown and enzymatic inhibitors of EZH2 on biological outcome have been described before: it was reported that catalytic inhibition of EZH2 using GSK343 and GSK126 induced no or modest expression of interferon gamma receptor 1 despite effective inhibition of H3K27me3 in a prostate cancer cell line, in contrast to depletion of EZH2 expression [45]. Similarly, it was found that SWI/SNF-mutant cancer lines are more sensitive to *EZH2* knockdown than catalytic inhibitors [46]. Regarding the autophagy context, the accumulation of LC3B-II may indicate that EZH2 inhibitors induce autophagy in CM cells. Although induction of autophagy may increase or repress cell survival depends on specific conditions, Hsieh et al. have shown that autophagy induced by GSK343 and UNC1999 occurred independently of EZH2 inhibition and promoted cell death in colorectal cancer cells [40]. This may explain why *EZH2* knockdown and UNC1999 treatment have partly distinct effects.

Our newly-developed zebrafish xenograft let tumor cells disseminate, and therefore served as an efficient metastatic model. After inoculation into the blood circulation, tumor cells spread to the head and tail of the zebrafish and proliferated, allowing further drug tests. GSK503 was not toxic to the fish, and like the results *in*

vitro, it profoundly reduced the growth of CM cells at a well-tolerated concentration. To the best of our knowledge, this is the first report using an animal model to test an epigenetic inhibitor in CM.

Overall, our results demonstrate that EZH2 is overexpressed in CM and lymph node metastases compared to normal conjunctival melanocytes and PAM, and high EZH2 protein levels are associated with tumor thickness. Both pharmaceutical compounds as well as RNAi targeting EZH2 repressed the growth of CM cells in culture and *in vivo*. Taken together, these data reveal that EZH2-targeted therapy may be a potential therapeutic strategy for patients with CM.

Acknowledgements

We thank Marja van Eggermond (IHB, LUMC, The Netherlands) for providing information regarding EZH2 and H3K27me3 antibodies, and Catalina Gomez Puerto (MCB, LUMC, The Netherlands) for sharing anti-p62 and anti-LC3B-II antibodies. And we appreciate that Robert M. Verdijk (Department of Pathology, Erasmas MC, The Netherlands) for providing metastases materials.

Abbreviations

Enhancer of zeste homolog 2 (EZH2), conjunctival melanoma (CM), polycomb repressive complex 2 (PRC2), trimethylation of lysine 27 in histone H3 (H3K27me3), immunohistochemistry (IHC), room temperature (RT), bovine serum albumin (BSA), phosphate buffered saline (PBS), staining index (SI), polyvinylidene difluoride (PVDF), horseradish peroxidase (HRP).

Conflict of interests

The authors declare no conflict of interest.

Grant support

This work was supported partly by grants from the China Scholarship Council (JC, 201206170141), the Dutch Cancer Society (UL 2013-5757), the LUMC MD/PhD programme grant (NJB), the Horizon2020 CURE UM 667787, and the National Council of Technological and Scientific Development CNPQ (Brazil, KCP).

Author contributions

MJJ initiated the idea, obtained funding and critically revised the article. AGJ participated in setting up, performing the experiments, and revising the manuscript. JC performed the *in vitro* experiments, analyzed the results and wrote the manuscript. KCP and AG established the animal model and did *in vivo* study. RCH and AFT was involved in *in vitro* experiments, and ESJ scored the slides. NJB collected clinical information and performed statistical analyses. MM and SD gave technical and material support.

References

1. Tuomaala S, Eskelin S, Tarkkanen A, *et al*. Population-based assessment of clinical characteristics predicting outcome of conjunctival melanoma in whites. *Invest Ophthalmol Vis Sci* 2002; 43: 3399-3408.

2. Yu GP, Hu DN, McCormick S, *et al*. Conjunctival melanoma: is it increasing in the United States? *Am J Ophthalmol* 2003; 135: 800-806.

3. Triay E, Bergman L, Nilsson B, *et al*. Time trends in the incidence of conjunctival melanoma in Sweden. *Br J Ophthalmol* 2009; 93: 1524-1528.

4. Shields CL, Shields JA, Gunduz K, *et al*. Conjunctival melanoma: risk factors for recurrence, exenteration, metastasis, and death in 150 consecutive patients. *Arch Ophthalmol* 2000; 118: 1497-1507.

5. Missotten GS, Keijser S, De Keizer RJ, *et al*. Conjunctival melanoma in the Netherlands: a nationwide study. *Invest Ophthalmol Vis Sci* 2005; 46: 75-82.

6. Werschnik C, Lommatzsch PK. Long-term follow-up of patients with conjunctival melanoma. *Am J Clin Oncol* 2002; 25: 248-255.

7. Griewank KG, Westekemper H, Murali R, *et al*. Conjunctival melanomas harbor BRAF and NRAS mutations and copy number changes similar to cutaneous and mucosal melanomas. *Clin Cancer Res* 2013; 19: 3143-3152.

8. Cao J, Heijkants RC, Jochemsen AG, *et al*. Targeting of the MAPK and AKT pathways in conjunctival melanoma shows potential synergy. *Oncotarget* 2016; 8: 58021-58036.

9. Pahlitzsch M, Bertelmann E, Mai C. Conjunctival melanoma and BRAF inhibitor therapy. *J Clin Exp Ophthalmol* 2014; 5: 322. doi: 10.4172/2155-9570.1000322.

10. Maleka A, Åström G, Byström P, *et al*. A case report of a patient with metastatic ocular melanoma who experienced a response to treatment with the BRAF inhibitor vemurafenib. *BMC Cancer* 2016; 16: 634.

11. Varambally S, Dhanasekaran SM, Zhou M, *et al*. The polycomb group protein EZH2 is involved in progression of prostate cancer. *Nature* 2002; 419: 624-629.

12. Bachmann IM, Halvorsen OJ, Collett K, *et al*. EZH2 expression is associated with high proliferation rate and aggressive tumor subgroups in cutaneous melanoma and cancers of the endometrium, prostate, and breast. *J Clin Oncol* 2006; 24: 268-273.

13. Ciferri C, Lander GC, Maiolica A, *et al*. Molecular architecture of human polycomb repressive compex 2. *eLife* 2012; 1: e00005. doi: 10.7554/eLife.00005.

14. Riquelme E, Behrens C, Lin HY, *et al*. Modulation of EZH2 expression by MEK-ERK or PI3K-AKT signaling in lung cancer is dictated by different KRAS oncogene mutations. *Cancer Res* 2016; 76: 675-685.

15. Konze KD, Ma A, Li F, *et al*. An orally bioavailable chemical probe of the Lysine Methyltransferases EZH2 and EZH1. *ACS Chem Biol* 2013; 8: 1324-1334.

16. Tiffen J, Gallagher SJ, Hersey P. EZH2: an emerging role in melanoma biology and strategies for targeted therapy. *Pigment Cell Melanoma Res* 2015; 28: 21-30.

17. Zingg D, Debbache J, Schaefer SM, *et al*. The epigenetic modifier EZH2 controls melanoma growth and metastasis through silencing of distinct tumor suppressors. *Nat Commun* 2015; 6: 6051. doi: 10.1038/ncomms7051.

18. Kim KH, Roberts CW. Targeting EZH2 in cancer. *Nat Med* 2016; 22: 128-133.

19. Knutson SK, Wigle TJ, Warholic NM, *et al*. A selective inhibitor of EZH2 blocks H3K27 methylation and kills mutant lymphoma cells. *Nat Chem Biol* 2012; 8: 890-896.

20. Bradley WD, Arora S, Busby J, *et al*. EZH2 inhibitor efficacy in non-Hodgkin's lymphoma does not require suppression of H3K27 monomethylation. *Chem Biol* 2014; 21: 1463-1475.

21. Edge SB, Byrd DR, Compton CC, *et al* (eds). Malignant melanoma of the conjunctiva. In AJCC Cancer Staging Manual 7th edn. 2010; pp 539–546. Springer: New York, NY.

22. Cao J, Brouwer NJ, Richards KE, *et al*. PD-L1/PD-1 expression and tumor-infiltrating lymphocytes in conjunctival melanoma. *Oncotarget* 2017; 8: 54722-54734.

23. Reijm EA, Timmermans AM, Look MP, *et al*. High protein expression of EZH2 is related to unfavorable outcome to tamoxifen in metastatic breast cancer. *Ann Oncol* 2014; 25: 2185-2190.

24. Nareyeck G, Wuestemeyer H, von der Haar D, *et al*. Establishment of two cell lines derived from conjunctival melanomas. *Exp Eye Res* 2005; 81: 361-362.

25. Keijser S, Maat W, Missotten GS, *et al*. A new cell line from a recurrent conjunctival melanoma. *Br J Ophthalmol* 2007; 91: 1566-1567.

26. Carlotti F, Bazuine M, Kekarainen T, *et al*. Lentiviral vectors efficiently transduce quiescent mature 3T3-L1 adipocytes. *Mol Ther* 2004; 9: 209-217.

27. Lawson ND, Weinstein BM. In vivo imaging of embryonic vascular development using transgenic zebrafish. *Dev Biol* 2002; 248: 307-318.

28. White RM, Sessa A, Burke C, *et al*. Transparent adult zebrafish as a tool for in vivo transplantation analysis. *Cell Stem Cell* 2008; 2: 183-189.

29. Schneider CA, Rasband WS, Eliceiri KW. NIH Image to ImageJ: 25 years of image analysis. *Nat Methods* 2012; 9: 671-675.

30. Pontes KC, Groenewoud A, Cao J, *et al.* Evaluation of (fli:GFP) Casper zebrafish embryos as a model for human conjunctival melanoma. *Invest Ophthalmol Vis Sci* 2017; in press.

31. R Core Team. R: A language and environment for statistical computing. 2013. R Foundation for Statistical Computing, Vienna, Austria. URL http://www.R-project.org/

32. Chou TC, Martine N. ComboSyn Inc Paramus NJ. 2005. CompuSyn for drug combinations. pc software and user's guide.

33. Barsotti AM, Ryskin M, Zhong W, *et al*. Epigenetic reprogramming by tumor-derived EZH2 gain-of-function mutations promotes aggressive 3D cell morphologies and enhances melanoma tumor growth. *Oncotarget* 2015; 6: 2928-2938.

34. Xu B, On DM, Ma A, *et al*. Selective inhibition of EZH2 and EZH1 enzymatic activity by a small molecule suppresses MLL-rearranged leukemia. *Blood* 2015; 125: 346-357.

35. Fan T, Jiang S, Chung N, *et al*. EZH2-dependent suppression of a cellular senescence phenotype in melanoma cells by inhibition of p21/CDKN1A expression. *Mol Cancer Res* 2011; 9: 418-429.

36. Xia H, Zhang W, Li Y, *et al*. EZH2 Silencing with RNA interference induces G2/M arrest in human lung cancer cells in vitro. *Biomed Res Int* 2014. doi: 10.1155/2014/348728.

37. Sha MQ, Zhao XL, Li L, *et al*. EZH2 mediates lidamycin-induced cellular senescence through regulating p21 expression in human colon cancer cells. *Cell Death Dis* 2016; 7: e2486.

38. Wei FZ, Cao Z, Wang X, *et al*. Epigenetic regulation of autophagy by the methyltransferase EZH2 through an MTOR-dependent pathway. *Autophagy* 2015; 11: 2309-2322.

39. Mizushima N, Yoshimori T. How to interpret LC3 immunoblotting. *Autophagy* 2007; 3: 542-545.

40. Hsieh YY, Lo HL, Yang PM. EZH2 inhibitors transcriptionally upregulate cytotoxic autophagy and cytoprotective unfolded protein response in human colorectal cancer cells. *Am J Cancer Res* 2016; 6: 1661-1680.

41. van der Ent W, Burrello C, Teunisse AF, *et al*. Modeling of human uveal melanoma in zebrafish xenograft embryos. *Invest Ophthalmol Vis Sci* 2014; 55: 6612-6622.

42. McHugh JB, Fullen DR, Ma L, *et al*. Expression of polycomb group protein EZH2 in nevi and melanoma. *J Cutan Pathol* 2007; 34: 597-600.

43. Lee ST, Li Z, Wu Z, *et al*. Context-specific regulation of NF-kB target gene expression by EZH2 in breast cancers. *Mol Cell* 2011; 43: 798-810.

44. Xu K, Wu ZJ, Groner AC, *et al*. EZH2 oncogenic activity in castration-resistant prostate cancer cells is Polycomb-independent. *Science* 2012; 338: 1465-1469.

45. Wee ZN, Li Z, Lee PL, *et al*. EZH2-mediated Inactivation of IFN-g-JAK-STAT1 signaling is an effective therapeutic target in MYC-driven prostate cancer. *Cell Rep* 2014; 8: 204-216.

46. Kim KH, Kim W, Howard TP, *et al*. SWI/SNF-mutant cancers depend on catalytic and non-catalytic activity of EZH2. *Nat Med* 2015; 21: 1491-1496.

Supplementary information

Supplementary Table 1. Primary antibodies for IHC.

Antibody	Specificity	Isotype	Company	Catalogue	Dilutions
EZH2	mouse	IgG1	BD Biosciences	612667	1:1000
H3K27me3	rabbit	IgG	Millipore	07-449	1:1000
Histone 3	mouse	IgG1	Cell signaling Technology (CST)	3638	1:1000
p21	mouse	IgG2bκ	Millipore	05-655	1:1000
PARP	rabbit	IgG	CST	9542	1:1000
LC3B	mouse	IgG1	NanoTools	0231-100	1:1000
USP7	mouse	IgG	Bethyl Laboratories	A300-033A	1:1000
γ-Tubulin	mouse	IgG1	Sigma-Aldrich	T6557	1:1000
Vinculin	mouse	IgG1	Sigma-Aldrich	V9131	1:1000

Supplementary Table 2. An overview of primers.

Primers	Forward	Reverse
p14ARF	TGATGCTACTGAGGAGCCAGC	ACCACCAGCGTGTCCAGGAA
p21	AGCAGAGGAAGACCATGTGGA	AATCTGTCATGCTGGTCTGCC
p16	AGCAGCATGGAGCCTTCGG	CGTAACTATTCGGTGCGTTGGG
p27	CAAATGCCGGTTCTGTGGAG	TCCATTCCATGAAGTCAGCGATA
CAPNS1	ATGGTTTTGGCATTGACACATG	GCTTGCCTGTGGTGTCGC
SRPR	CATTGCTTTTGCACGTAACCAA	ATTGTCTTGCATGCGGCC

Supplementary Table 3. Clinical information of patients.

Study number	Sex	Age at diagnosis (yr)	Follow-Up (months)	Local Recurrence	Time to recurrence (months)	Metastases	Time to metastasis (months)	Location of Metastases	Status	Location on Conjunctiva	Thickness (mm)	Largest Basal Diameter (mm)	cTNM (7th ed)	EZH2 score	EZH2 category
1	Female	59	43.6	No		No			Alive	Non-epibulbar	1.2	8	2	4	High
2	Female	47	246.8	Yes	48.9	No			Alive	Epibulbar	0.6	12	1	0	Low
3	Male	64	78.6	Yes	24.6	No			Alive	Epibulbar	0.3	7	1	4	High
4	Female	84	42.3	No		Yes	27	Distant skin	Death due to metastases	Non-epibulbar	6	20	2	6	High
5	Male	61	51.9	No		No			Alive	Non-epibulbar	1.4	17	2	1	Low
6	Female	21	50.5	No		No			Alive	Epibulbar	0.6	5	1	1	Low
7	Male	46	6.7	No		No			Alive	Non-epibulbar	2.5	30	2	2	Low
8	Male	33	107.6	Yes	37.8	No			Alive	Epibulbar	0.2	6	1	2	Low
9	Male	42	61.3	No		No			Alive	Epibulbar	Unknown	2	1	0	Low
10	Female	69	35	No		No			Alive	Non-epibulbar	16	16	2	9	High
11	Male	58	64.9	No		No			Alive	Epibulbar	4	13	1	4	High
12	Female	49	37.3	No		No			Alive	Non-epibulbar	4.2	10	2	4	High
13	Female	72	56.1	No		No			Alive	Epibulbar	0.3	15	1	2	Low
14	Female	84	3.3	No		No			Death due to unknown cause	Epibulbar	4	15	1	9	High
15	Female	73	37.2	No		No			Alive	Epibulbar	0.8	7	1	0	Low
16	Male	60	98.3	Yes	70.3	Yes	91.9	Brain. multiple visceral	Death due to metastases	Epibulbar	Unknown	5	1	1	Low
17	Female	67	45.7	No		No			Alive	Epibulbar	1.2	12	1	4	High
18	Female	56	23.8	No		No			Alive	Epibulbar	0.2	5	1	6	High
19	Male	56	34.2	Yes	32.7	No			Alive	Epibulbar	0.2	12	1	1	Low
20	Female	56	27.1	Yes	8.5	No			Alive	Epibulbar	2.5	Unknown	1	6	High
21	Female	75	41.9	Yes	8.4	No			Death due to unknown cause	Epibulbar	5	Unknown	1	4	High
22	Female	40	58.1	Yes	34.8	No			Alive	Epibulbar	1	9	1	2	Low
23	Female	86	12.8	No		No			Alive	Epibulbar	0.1	6	1	6	High
24	Male	68	46.4	Yes	17.8	No			Alive	Epibulbar	0.2	2	1	2	Low
25	Male	68	29.5	No		No			Alive	Epibulbar	0.2	12	1	2	Low
26	Male	80	52.4	Yes	42.1	Yes	51.4	Unknown	Death due to metastases	Non-epibulbar	Unknown	Unknown	2	6	High

Supplementary Table 4. EZH2 score of PAM.

Study number	Atypia	EZH2 score	EZH2 category
PAM1	Mild	0	low
PAM2	Unknown	0	low
PAM3	Mild	0	low
PAM4	Mild	0	low
PAM5	Mild	0	low
PAM6	Mild	0	low
PAM7	Severe	0	low
PAM8	Moderate	0	low
PAM9	Mild	0	low

PAM: Primary acquired melanosis.

Supplementary Table 5. EZH2 score of lymph node metastases.

Study number	EZH2 score	EZH2 category
M1	3	low
M2	4	high
M3	6	high
M4	9	high
M5	4	high
M6	6	high
M7	9	high
M8	6	high

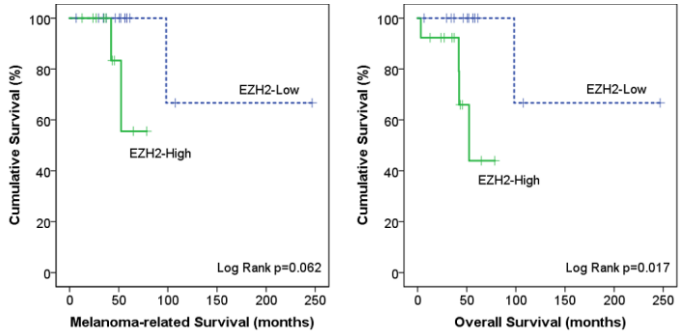

Supplementary Figure 1. Kaplan-Meier survival curves based on low and high EZH2 expression in CM groups of 26 patients. Left: melanoma-related survival. Right: overall survival.

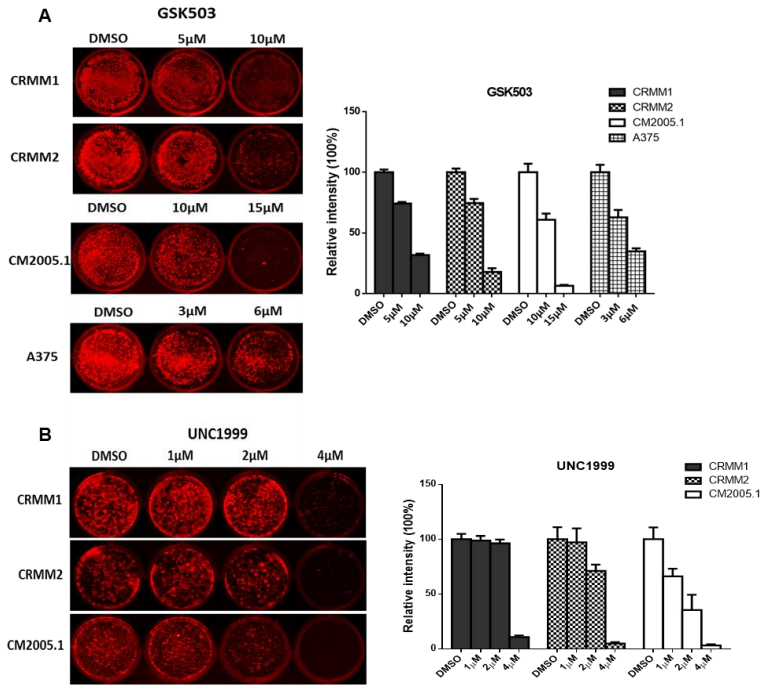

Supplementary Figure 2. GSK503 and UNC1999 inhibit colony formation in melanoma cell lines. Left: Representative images of cells exposed to drugs for 2 weeks. Right: Corresponding statistical analysis of colony formation. Error bars represent SEM. Data are presented as means ± SEM, from one representative experiment.

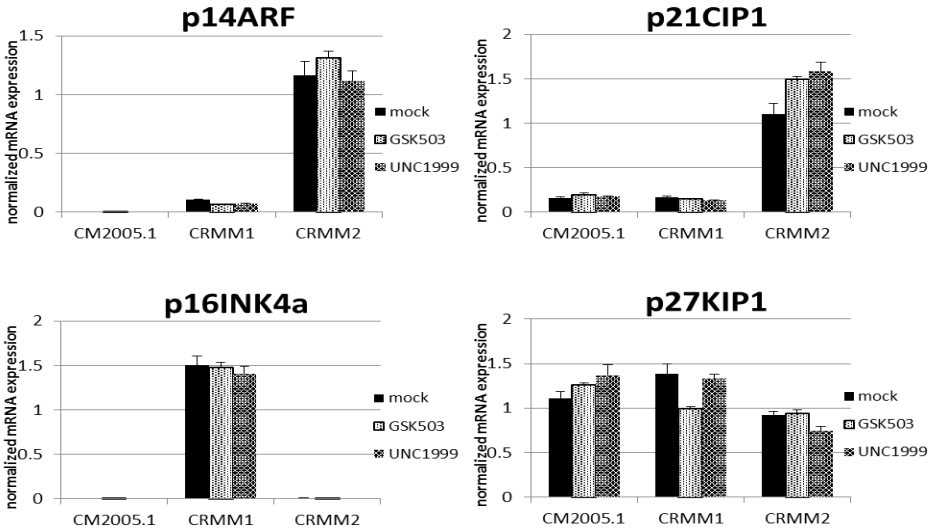

Supplementary Figure 3. GSK503 and UNC1999 don't alter the mRNA levels of p14ARF, p16, p21 or p27 in CM cell lines. Three CM cell lines were treated with GSK503 or UNC1999, and the relative expression was obtained by normalizing to housekeeping genes CAPNS1 and SRPR.

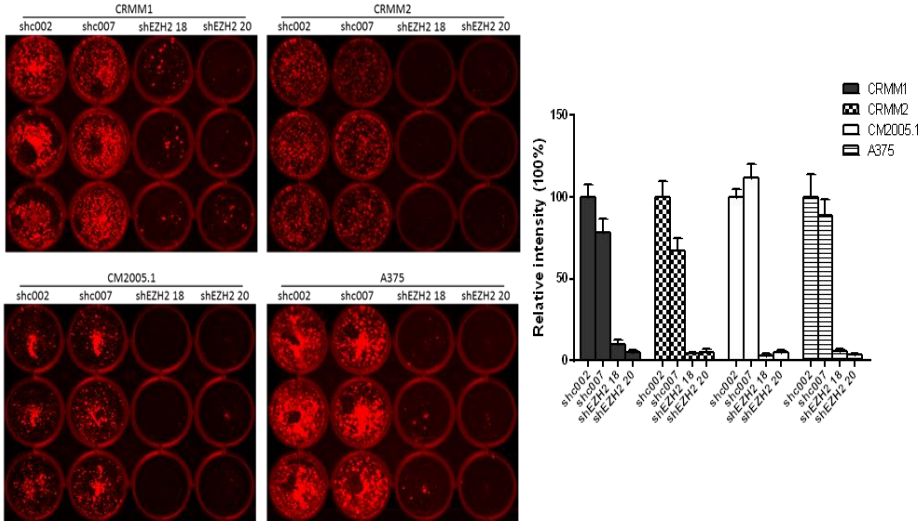

Supplementary Figure 4. EZH2 depletion inhibits colony-formation of three CM cell lines and A375. Cells were seeded in triplicate in 12-well plates. After 2-week incubation with siRNA, the plates were scanned. The intensity (Y axis) was normalized to shc002 control cells in each experiment. Data represent means ± SEM.

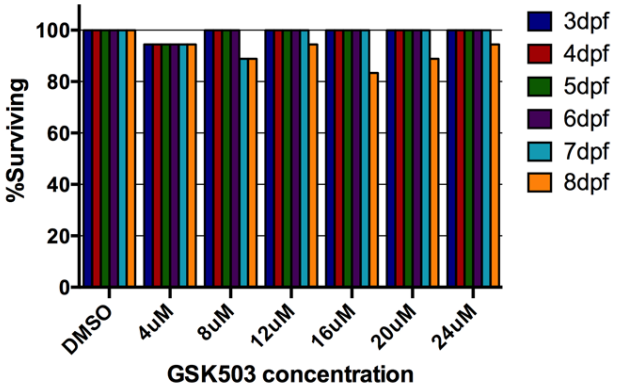

Supplementary Figure 5. Toxicity test of GSK503 in zebrafish. Toxicity test performed in non-injected (fli: GFP) Casper zebrafish embryos from 3 dpf until 8dpf, using different concentrations of GSK503. A concentration with a survival equal or higher than 80% was considered nontoxic to the embryos.